Original Research

Phase-Contrast Echo-Planar MR Imaging: Real-Time Quantification of Flow and Velocity Patterns in the Thoracic Vessels Induced by Valsalva's Maneuver

A. C. Eichenberger, MD BSEE • J. Schwitter, MD • G. C. McKinnon, PhD • J. F. Debatin, MD
G. K. von Schulthess, MD PhD

Although the clinical manifestations of Valsalva's maneuver are well known, the associated hemodynamic changes in the great vessels have not been extensively studied and documented. In each of six healthy subjects, we evaluated three "quasi-steady-state" phases of Valsalva's maneuver: (1) during normal respiration, (2) during late strain, and (3) 4 seconds after strain release. Continuous flow, velocity, and cross-sectional area measurements were obtained in the superior vena cava, pulmonary trunk, and thoracic aorta with single-shot echo-planar MR imaging (EPI) with velocity-encoded gradients, which provided 256 images in 5 seconds, yielding 26 velocity-encoded images per second. In the superior vena cava, Valsalva's maneuver induced an 11% decrease in average flow volume, a 102% increase in peak flow velocity, a 156% increase in the time velocity integral, and a 37% decrease in cross-sectional area. MR velocity measurements agreed with echocardiographic data and supplied additional information on flow and morphology. EPI showed a reduction in venous return during Valsalva's maneuver by simultaneously assessing flow, velocity, and vessel morphology; this technique appears to be useful in the analysis of flow dynamics of the great vessels.

JMRI 1995; 5:648–655

Abbreviations: EPI = echo-planar imaging, FOV = field of view, PAT = pulmonary arterial trunk, SVC = superior vena cava

From the Department of Medical Radiology, University Hospital, CH-8091, Zürich, Switzerland (A.C.E., J.S., G.C.McK, J.F.D., G.K.vS.). Received March 6, 1995; revision requested April 25; revision received June 15; accepted June 16. **Address reprint requests to** A.C.E.

TRADITIONALLY, BLOOD FLOW quantification has been performed by cardiac catheterization studies (1), and more recently by Doppler sonography (2,3). Both techniques have the severe limitation that the flow velocity and vessel cross-sectional area cannot be assessed simultaneously. Specifically, catheter studies require steady-state conditions for flow measurements and cannot be performed routinely on volunteers, owing to their invasiveness and to the fact that they exposure patients to X-rays. Sonography is limited by the acoustic window and geometric considerations.

Important physiologic phenomena, such as the cardiovascular response to Valsalva's maneuver, have not been fully accessible to noninvasive studies in humans. Hence, the cardiovascular effects of this maneuver, in which subjects close their nose and mouth and then press forcibly to increase the intrathoracal pressure, could not be studied in full. The normal hemodynamic response to Valsalva's maneuver is characterized by a gradual decrease in arterial pressure, pulse pressure, and stroke volume accompanied by tachycardia. Following release of strain, a reflectory "overshoot" of the systemic arterial pressure and stroke volume is accompanied by bradycardia. The response to Valsalva's maneuver has long been used to evaluate cardiac function (4,5). Although many studies have documented the changes associated with Valsalva's maneuver, there is little documentation of transient blood flow patterns in the great vessels. In particular, there have been no simultaneous measurements of flow velocity, vessel cross-sectional area, and flow during an interventional maneuver, and a study quantifying the transient flow volume of venous return to the right side of the heart during strain has not been done. Hence, evidence of these phenomena has been circumstantial.

MR imaging has received increasing attention as a noninvasive means to assess physiologic and pathologic flow states, because it is exquisitely sensitive to flow and motion. With the use of phase-mapping techniques, many studies (6–9) have demonstrated that MR imaging is the most accurate in vivo noninvasive technique to quantify flow in the human vessel system. Conventional MR phase-contrast techniques acquire data averaging

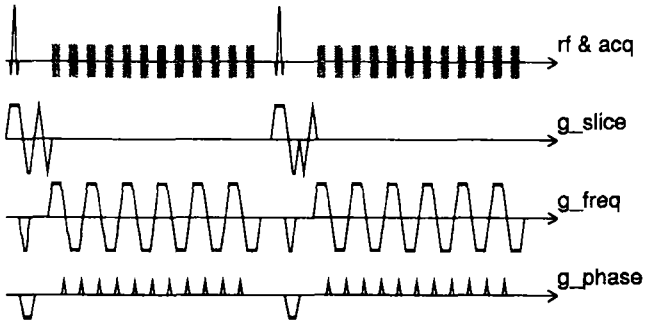

Figure 1. Diagram of the phase-contrast single-shot gradient EPI sequence. rf = radio frequency pulse, g_slice = slice selection and velocity-encoded gradient.

over many cardiac and respiratory cycles. This averaging of flow velocities has been seen as an advantage because any short-term variability of flow does not introduce gross errors in measurement. However, disadvantages are equally great; for example, heart patients, suffering from arrhythmias or dyspnea, cannot be adequately examined. Furthermore, short-term variations in flow—such as in response to exercise, pharmacologic stress, or respiration and interventional maneuvers—cannot be assessed. In these situations, rapid data acquisition is required to characterize transient blood flow phenomena.

Since the advent of fast-switching gradient power supplies, the speed with which MR images can be acquired has improved greatly, and attempts have been made to quantify blood flow with the use of EPI (10–15). Quantification of pulsatile flow requires simultaneous and adequate temporal and spatial resolution. In essence, an increase in temporal resolution will decrease image spatial resolution and vice versa. Theoretical analysis (16,17) shows that if the pixel length is 25% or less of the vessel diameter, then a flow error of approximately 10% results. Hence, using relatively low spatial resolution, real-time phase-mapping EPI should provide adequate temporal and spatial resolution to quantitatively evaluate velocity and flow in the large vessels of the thorax. In this study, we applied such a technique to the analysis of the hemodynamic phenomena associated with Valsalva's maneuver. Flow in the superior vena cava (SVC), the thoracic aorta, and the pulmonary arterial trunk (PAT) were examined with phase-mapping EPI, and the data obtained were compared with data from the literature, when available.

• MATERIALS AND METHODS

Measurements were obtained in six volunteers, 22–35 years old, who were lying supine in the MR system. None had evidence of cardiovascular disease. The volunteers were instructed to perform Valsalva's maneuver, and imaging was done during three "quasi-steady-state" phases of Valsalva's maneuver: during normal breathing, during late strain, and 4 seconds after release of strain. Flow measurements were acquired in the ascending aorta, the descending aorta, the SVC, and the PAT for approximately 5 seconds (see below). Additional measurements at the level of the PAT, which were obtained in five subjects during the release of strain, allowed observation of the impulsive flow behavior in the great vessels. This was necessary because whereas, for anatomic reasons, the ascending aorta, descending aorta, and SVC could be visualized simultaneously, the anatomic relation of the PAT was more variable and sections where the ascending aorta and PAT were close to perpendicular to the imaging slice were difficult to obtain.

All measurements were performed in the body coil of a GE Signa Advantage 1.5-T imaging system (Buc, France) equipped with the following additional hardware: a gradient accelerator unit on the x-axis, with a maximum gradient amplitude of 18 mT/m and a slew rate of 200 mT/m per msec. Additional performance enhancement on the y-axis gradient with a maximum amplitude of 15 mT/m and a maximum slew rate of 40 mT/m per msec. The z-axis had a conventional Signa Advantage gradient, with a maximum amplitude of 10 mT/m and a maximum slew rate of 20 mT/m per msec. The nonisotropic nature of the gradient system implied that only transaxial EPI was practical, and resulted in a substantial acceleration of imaging. The phase-contrast EPI technique had been validated on a flow phantom and in vivo in steady state (during normal respiration) as described previously (17–19) and is shown schematically in Figure 1. In this study, an interleaved EPI sequence (20–22) was applied in the simplest form to provide phase-contrast images. Single-shot EPI allows for the acquisition of the entire K-space after a single RF-pulse, thereby obtaining the fastest possible acquisition time for a given spatial resolution. To produce a velocity-encoded image with the phase-contrast method, an acquisition of the complete K-space data set must be repeated with the sign of the bipolar velocity-encoded gradient inverted in the second measurement (see g_slice in Fig 1). The positive and negative velocity-encoded data sets are acquired one after the other in the same heart cycle in a sequential fashion. Depending on the application, echo-planar images with high spatial resolution can be acquired in approximately 100 msec or, if high temporal resolution is needed, images can be obtained with low spatial resolution (16). On the basis of a theoretical analysis (16), it was shown that flow determinations accurate to better than 10% can be obtained as long as the pixel diameter length is 25% or less of the vessel diameter. For example, a 5 × 5 mm in-plane resolution using a 64 × 32 matrix with a rectangular field of view (FOV) of 32 × 16 cm was deemed acceptable for a vessel diameter of 20 mm. In this study, a trade-off between temporal and spatial resolution was applied. While maintaining the matrix size at 64 × 32, we used the smallest possible FOV for each subject that did not cause wraparound artifacts to superimpose on the examined vessels. In three of six subjects a rectangular FOV of 32 × 16 cm was applied, resulting in an in-plane resolution of 5 × 5 mm. With a 5 × 5 mm in-plane resolution for EPI acquisition, the repetition time (TR) was 18.5 msec with an effective echo time (TE) of 8.1, and, as phase-sensitive imaging requires a positive and a negative velocity-encoded image, which are subtracted, the total acquisition time per phase image was 37 msec. In the other three subjects, a rectangular FOV of 26 × 13 cm was applied, resulting in an in-plane resolution of 4 × 4 mm. With a 4 × 4 mm in-plane resolution for EPI acquisition, the TR was 21 msec with an effective TE of 8.7, which yielded a total acquisition time of 42 msec. The variable FOV allowed for a continuous optimization between temporal and spatial resolution. Short imaging times (18.5–21 msec) assured images free of motion artifacts without ECG gating or respiratory compensation. A half K-space acquisition was used with eight extra K-lines acquired in the other half of K-space; thus, a total of 24 K-lines

were acquired. The phase-contrast velocity-encoding constant was set at 200 cm/sec. A maximum of 256 echo-planar images (128 velocity-encoded images and 128 magnitude images) could be acquired in 4.8 seconds for an FOV of 32 cm, and in 5.4 seconds for an FOV of 26 cm. The data acquisition sampling rate was 200 kHz (one sample every 4 μsec). The excitation pulse (flip) angle was set at 25° in order to provide reasonable contrast between stationary tissue and flowing blood. Phase-contrast EPI flow measurements have previously been validated in vivo as compared with conventional cine phase-contrast MR images, showing excellent correlation (r = .98) for steady-state conditions (17).

Using both the velocity-encoded and the corresponding magnitude images, we estimated flow, maximum velocity, and vessel cross-sectional area interactively on a SUN Sparc II workstation (SUN Microsystems, Zürich Switzerland). Estimation involved placing a region of interest (ROI) approximately surrounding the vessel of interest on the magnitude and/or velocity-encoded image. A magnitude threshold of 35% of the maximum amplitude was chosen to delineate the vessel within the ROI. All pixels within the ROI that had an amplitude above the threshold were automatically marked. The absolute flow was calculated by adding the velocities of the marked pixels and by multiplying the summed velocities by the area of one pixel. The cross-sectional area was calculated by adding the area of the marked pixels. The maximum velocity corresponded to the marked pixel with maximum absolute velocity. Average flow velocity was calculated by dividing the flow by the cross-sectional area. This process was repeated for each image. However, if there was no significant displacement of the vessel of interest from one image analyzed in the series to the next, the ROI from the preceding phase was automatically assigned to the next image. This automation, by which the ROI did not need to be adjusted from one image to the next, greatly reduced the operator-dependent interactions.

Quantitative and qualitative analyses of flow, velocity, and cross-sectional area curves were performed. As no ECG gating was recorded, the end points of the cardiac cycle were defined on the flow curve of the ascending aorta; the local minimum flow before the ventricular ejection was used as the end point of the cardiac cycle. For the estimation of cardiac parameters in the quasi–steady states of Valsalva's maneuver, all complete cardiac cycles in the scan were averaged by using these defined end points. Internal consistency was controlled by comparing the cardiac output measured in the ascending aorta with the cardiac output simultaneously measured in the pulmonary trunk. The significance of changes in these parameters was evaluated by applying Student's t-test. Analysis of time-velocity curves was conducted by comparing peak velocities and time-velocity integrals obtained by using real-time EPI data with those obtained by using percutaneous and intravascular sonography.

• RESULTS

Approximately 6,000 magnitude and velocity-encoded images were reconstructed and evaluated. Figure 2 shows corresponding images obtained at a level at which the ascending aorta is close to perpendicular to the transaxial slice in a single subject in two quasi–steady states of Valsalva's maneuver. Despite the relatively low spatial resolution of the single-shot echo-planar images, interactive identification of the great vessels posed no difficulties. Imaging and flow quantification

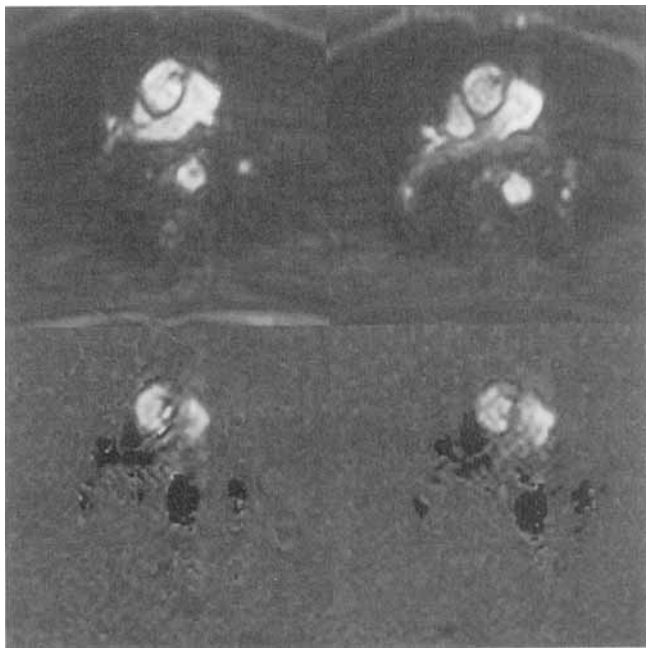

Figure 2. Magnitude (top) and corresponding magnitude-weighted velocity-encoded images (bottom) at the level of the ascending aorta acquired in 42 msec during systole for two different quasi–steady states of Valsalva's maneuver for a single subject. The images to the left were acquired during late strain, those to the right after release of strain. Almost total collapse of the SVC was noted during the strain phase, whereas an increase in cross-sectional area was observed after release of strain.

succeeded for all subjects in the ascending and descending aorta and the superior vena cava during the three quasi–steady states of Valsalva's maneuver. For geometric and anatomic reasons, simultaneous imaging of the ascending aorta and PAT proved to be more difficult, succeeding in three subjects during normal respiration, in two subjects during strain, in two subjects during release of strain, and in no subjects after strain release. Hence, the transaxial slice, which is perpendicular to the ascending aorta and the PAT, requires two imaging planes in most subjects. The data show that such simultaneous imaging is more difficult when an exercise like Valsalva's maneuver is performed, because it causes the vessels to change their relative position; in particular, the PAT is known to vary greatly in location with different flow states.

Although our main focus was on the SVC, data on the ascending aorta, descending aorta, and PAT were also evaluated, serving as internal consistency checks and yielding data that can be compared with published findings. In Figure 3, we show the data from a single subject during normal breathing. Consistent with existing physiologic data, the peak flow in the ascending aorta occurs earlier and exceeds that in the descending aorta. Although the onset of PAT flow is simultaneous to that in the ascending aorta, the peak occurs later and anterograde flow occurs throughout the cardiac cycle. The temporal resolution was sufficient to capture not only the period of flow reversal in the ascending aorta at end systole, corresponding to aortic valve closure, but also the anterograde motion of the ascending aorta during atrial contraction and the very short retrograde motion during the isovolumetic ventricular contraction.

Real-time flow, velocity, and cross-sectional area measurements for the SVC and flow measurements for

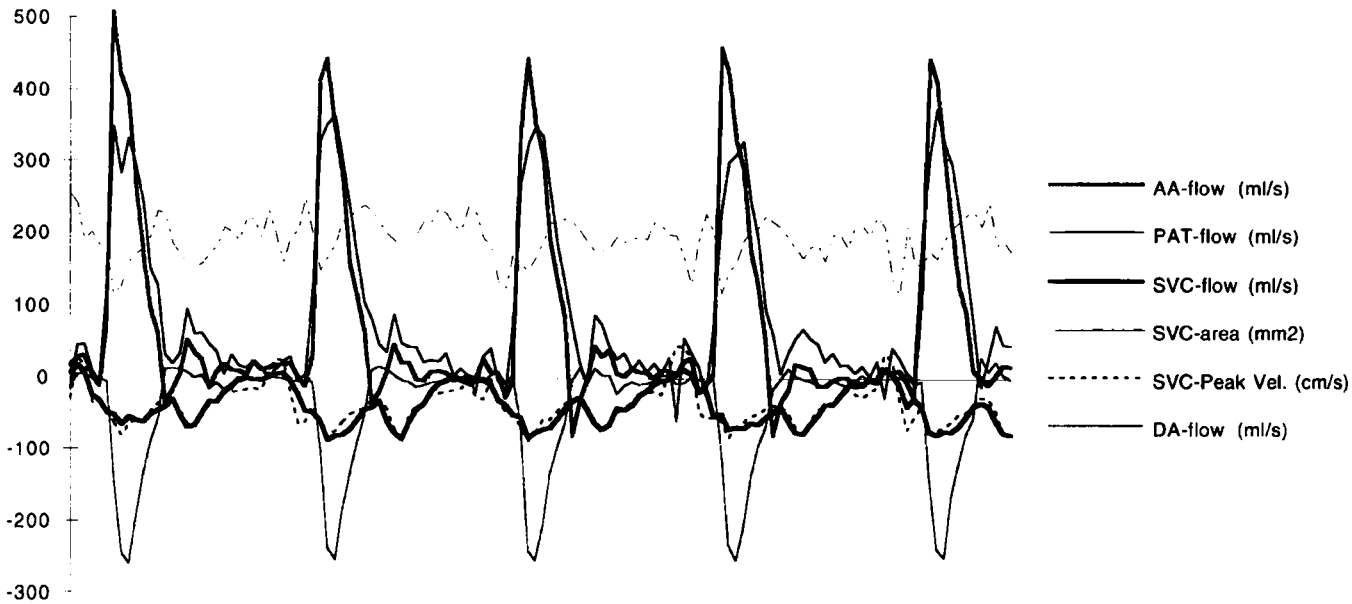

Figure 3. Flow, velocity, and cross-sectional area for the SVC and the simultaneously measured flow curves for the ascending aorta, descending aorta, and pulmonary trunk for a single subject during normal breathing are shown for a period of 5.3 seconds. The high temporal resolution of the flow profiles allowed excellent characterization of the blood flow in both the ascending and descending aorta, the superior vena cava, and the pulmonary trunk.

the ascending aorta during three quasi-steady-state phases of Valsalva's maneuver are shown for an individual subject in Figure 4. The estimated data on flow, velocity, and area of the SVC and flow in the ascending aorta averaged among the subjects are summarized in Table 1.

In normal respiration, the flow quantification in the ascending aorta, averaged among the six subjects, yielded a stroke volume (SV) of 48 +/− 8 mL/m² and a cardiac output of 2.7 +/− 0.4 L/min per m², with a mean heart rate of 61 +/− 10 bpm (all values, mean + 1 SD). During late strain of Valsalva's maneuver, a significant decrease (of 25%) was observed in the stroke volume ($P < .01$), whereas the decrease in cardiac output (of 5%) was not significant ($P < .3$). The heart rate increased significantly, by 28% ($P < .001$) bpm. Four seconds after stain release, stroke volume and cardiac output increased significantly relative to normal respiration, by 35% ($P < .05$) and by 20% ($P < .025$), respectively; whereas the heart rate decreased insignificantly, by 2% ($P < .35$). The significance of changes in these parameters was evaluated by applying Student's *t*-test and are shown in Table 1. Simultaneous flow measurements in the ascending aorta and the PAT in three subjects (for a total of 14 heart cycles) during normal respiration revealed a relative cardiac output in the ascending aorta to the PAT of 95% +/− 6% (range, 94–100%). This physiologic left-to-right shunt agrees with the previously published value of 98%.

Data for the flow time curves of the ascending aorta, the SVC, and the PAT during the release of strain are shown in Figure 5. Strain release coincided with the beginning of the scan. Immediately after release of strain there was a rapid increase of anterograde flow in the SVC to a maximum instantaneous flow rate of 180 mL/min and a large increase of PAT flow, which reached a maximum in the third heart cycle, measuring 150% of the simultaneously measured flow in the ascending aorta in this subject. Immediately after release of strain, the flow in the aorta was reduced, corresponding to the transitory reduced filling of the left ventricle. In the fifth heart cycle, relative pulmonary and aortic flows were again roughly equal, whereby the aortic flow started to demonstrate the "overshoot" in the sixth heart cycle.

The most interesting and unique data were obtained for the SVC. As shown in Figure 2, the form of the SVC is variable. A substantial reduction in cross-sectional area of the SVC was noted during the late strain phase. Although the form of the SVC during normal respiration is close to circular, during late strain the SVC is pressed against the aorta and its form becomes more triangular.

In Figure 3, the flow velocity, cross-sectional area, and flow in the SVC are shown for normal respiration. The flow profile in the SVC is similar to the events observed when examining a normal jugular venous pulse and is characterized in all subjects during normal breathing by two anterograde maxima (with negative sign, relative aortic flow) and one retrograde minimum. The two anterograde maxima consist of one during systole, corresponding to the ventricle contraction and atrial filling (x wave of the jugular venous pulse), and the other peak during early diastole, corresponding to the reopening of the tricuspid valve and fast ventricular filling (y wave). The retrograde peak corresponds to atrial contraction (a wave). The local flow minimum between the x wave and the y wave (v wave) is observed during late ventricular systole with the tricuspid valve shut. The c wave, corresponding to the beginning of ventricular contraction (ballooning of the tricuspid valve) was observed in three (50%) of the subjects. The measured cross-sectional area of the SVC showed a strong variation within the heart cycle. However, the beat-to-beat variation in average cross-sectional area was relatively small.

The real-time velocity, area, and flow curves of the SVC during the three quasi-steady states of Valsalva's maneuver are shown for an individual subject in Figure 4, and the averaged estimated data on the six subjects are given in Table 1. The average area, velocity, and flow were recorded for each phase of the maneuver. Average area of the SVC for all subjects during normal

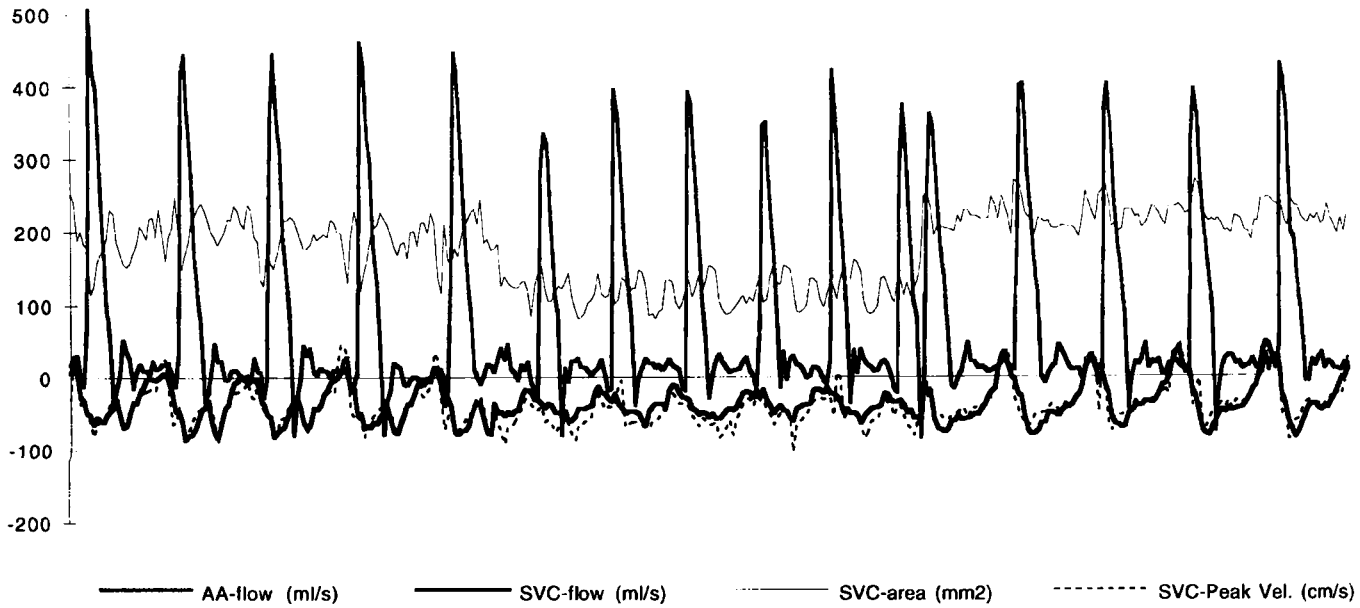

Figure 4. Blood flow, velocity, and cross-sectional area of the SVC and flow curves of the ascending aorta for a single subject as measured by EPI during three quasi-steady-state phases of Valsalva's maneuver. Each phase of the maneuver is measured for a period of 5.3 seconds: on the left side = normal, shallow breathing; in the middle = during late strain; and on the right = 4 seconds after strain release.

respiration was 198 +/− 22 mm^2, whereas it decreased to 125 +/− 35 mm^2 during strain ($P < .001$) and increased to 215 +/− 40 mm^2 ($P < .001$) after release of strain. The peak flow velocity doubled during late strain, but after strain release it remained high because of increased venous return (Table 1). By integrating the peak flow velocity curve over time, the time velocity integral was calculated for each subject and for each phase of Valsalva's maneuver. The peak flow velocity increased from 73 cm/sec to 150 cm/sec ($P < .001$), and the time velocity integral increased markedly during strain, from 25 cm to 63 cm ($P < .001$). Finally, the average flow of the SVC was estimated for each subject and for each phase of the maneuver; and, in contradistinction to the velocity, it decreased significantly (by 11%) during the late strain phase, from 42 mL/sec to 38 mL/sec ($P < .05$). Transient effects after strain release on the SVC are again reviewed in Figure 5. Immediately after strain release there was a rapid increase in anterograde flow in the SVC maintained over approximately three heart cycles to a maximum instantaneous flow rate of 180 mL/min in this subject (i.e., more than twice the peak flow rate in the SVC during normal respiration).

• DISCUSSION

The phase-contrast EPI technique described here is quite versatile, as it permits a flexible trade-off between temporal and spatial resolution. For the purposes of studying hemodynamic effects of Valsalva's maneuver, we were able to adjust the spatial resolution such that it was adequate for flow quantification and had sufficiently high temporal resolution for analyzing the complicated flow patterns of the SVC. Although various investigators have undertaken to quantify flow in various vessels, including the coronaries, only Firmin et al (14) have described a phase-contrast EPI method and have measured flow in the aorta, but not the SVC. In contrast, the EPI method presented in this study uses higher spatial and temporal resolution and is the first MR imaging technique to show real-time on-line data acquisition without gating.

To date, several research groups have demonstrated the combination of segmented K-space MR sequences combined with phase-contrast velocity-encoded gradients for the quantification of flow in vivo. The simplest form of the segmented K-space sequences is the single-shot EPI, which allows for the acquisition of the entire K-space after a single RF-pulse excitation. For the purpose of measuring flow in the great vessels, we choose the phase-contrast single-shot EPI technique for our flow measurements, because it achieves the fastest possible acquisition times, eliminating physiologic motion. However, it has been shown that single-shot EPI has limited spatial resolution in tissues with fast $T2^*$ decay and is subjected to motion artifacts because of long echo times (22). With limited spatial resolution it is difficult to obtain flow data in small vessels. The high motion sensitivity implies that small amounts of turbulent flow can result in signal loss, possibly reducing the accuracy of flow quantification. Nevertheless single-shot EPI flow measurements have been successfully undertaken. Firmin et al (14) used a phase-contrast method, Guilfoyle et al (15) have applied a prepulse for the velocity encoding, and Poncelet et al (10) have succeeded in measuring the flow in the coronary arteries using the time-of-flight effect. In our institution, we have conducted validation experiments of phase-contrast EPI on a flow phantom and in vivo (17) and studied the relationship between spatial resolution and flow error for phase-contrast MR imaging (16). The limited spatial resolution was not a significant problem in the flow measurements of the great vessels. The effects of turbulence in the physiologic realm have been shown to be negligible with the short echo times of 8.1–8.7 msec, as used in our study (6).

The cross-sectional area of the SVC showed strong fluctuations within the heart cycle. This fluctuation is certainly due in large part to the fluctuations in venous pulse pressure and the resulting cross-sectional area. However, the magnitude-dependent masking of vessels used in this study also reflects the variations in MR blood signal intensity, well known as the in-flow phe-

Table 1
Flow Data for the Ascending Aorta and Flow and Velocity Data for the Superior Vena Cava

	Ascending Aorta		
Quasi-Steady State	SV	CO	HR
Normal respiration	48 +/− 8	2.7 +/− 0.4	61 +/− 10
During late strain	36 +/− 6[a]	2.6 +/− 0.4[b]	79 +/− 15[c]
After strain release	56 +/− 12[d]	3.2 +/− 0.3[d]	59 +/− 8[b]

	Superior Vena Cava			
Quasi-Steady State	Average Flow	Peak Vel.	TVI	Avg. Area
Normal respiration	42 +/− 4.6	73 +/− 26	25 +/− 8.2	198 +/− 24
During late strain	38 +/− 6.2[d]	150 +/− 36[c]	63 +/− 14.6[c]	125 +/− 35[c]
After strain release	44 +/− 7.5[b]	135 +/− 35[c]	45 +/− 13.2[c]	215 +/− 40[c]

NOTE: Data were acquired during three quasi-steady state phases of Valsalva's maneuver during normal respiration; late strain; and 4 seconds after strain release. Values are averaged among all six subjects and are given as mean +/− ISO and the level of significance relative to values during normal respiration.
[a] = $P < .01$
[b] = not significant
[c] = $P < .001$
[d] = $P < .05$
SV = stroke volume (ml/m²), CO = cardiac output (L/min per mm²), HR = heart rate (bpm), average flow (mL/sec), Peak Vel. = peak flow velocity (cm/sec), TVI = time velocity integral (cm), Avg. Area = cross-sectional area of SVC (mm²).

nomenon. A magnitude threshold of 35% of the maximum amplitude was applied to all scans and subjects to delineate the vessel within the ROI. The 35% threshold was found to provide the optimal vessel delineation as judged visually by the operator. Higher threshold values usually showed an overestimation and lower threshold values an underestimation of vessel cross-sectional area. As shown in this study, the SVC is characterized by triphasic flow, giving rise to frequent fluctuations in blood in-flow and MR signal intensity. An alternative to a constant magnitude threshold in percent of maximum signal intensity is a threshold value fixed and independent of the intensity profile within the ROI. The fixed threshold gave similar results when applied to a single scan. Unfortunately, a fixed threshold must be found for each scan, since the average MR signal on the magnitude images showed considerable variation from scan to scan. An optimal, automated method for the estimation of vessel cross-sectional area remains an area for further research.

Although our main focus was on examining the SVC flow, measurements in the ascending aorta, descending aorta, and PAT were used to detect the consistency of the method and to demonstrate the known hemodynamic response to Valsalva's maneuver. The results of these measurements certify that the method used is accurate and that Valsalva's maneuver was properly performed. In particular, we showed that the relative flow between the ascending aorta and PAT was close to 1, with a well-known physiologic left-right shunt. That our average shunt value was 96% rather than 98% is of no concern in this small population.

This work shows that real-time phase-contrast EPI is capable of providing insights into physiologic flow events in the cardiovascular system, yielding a hitherto inaccessible wealth of information. With phase-contrast EPI it is possible to directly measure for the first time and noninvasively the transient flow behavior during an interventional maneuver. In particular, we could prove that SVC flow is indeed decreased during the strain phase of Valsalva's maneuver. To date, this observation of decreased flow has not been made directly by MR imaging or by any other imaging technique, such as sonography and invasive heart catheterization.

Sonography has difficulty in simultaneously assessing velocity and cross-sectional vascular area. Increased peak flow during strain has been documented with sonography, but this technique cannot simultaneously assess cross-sectional area and velocity, and the consequent condition that venous return in the SVC is reduced during strain. When comparing the EPI data with published studies on sonographic data during strain (23,24), the measured values for flow velocity and time velocity integral show good agreement. Using percutaneous sonography, researchers detected in 13 healthy subjects an increase in the flow velocity integral from 17 cm at rest to 61 cm during late strain (23). A technically adequate sonographic measurement of the SVC diameter during strain was successful in only five of 13 subjects. The cross-sectional area of the SVC could not be adequately measured by percutaneous sonography. Other researchers, using intravascular sonography, detected a cross-sectional area of the SVC of 180 mm² at rest and 90 mm² during strain (24). Intravascular sonography could not quantify the flow velocities. Sonography requires two distinct measurements: flow-velocity and vessel diameter. Vessel diameter allows the estimation of cross-sectional area only after geometric assumptions. Technically adequate assessment by sonography of any diameter of the SVC during strain is not attainable in most subjects (23). It is of interest to point out that the form of the SVC is variable, and certainly most often not circular. Thus, the diameter of the SVC is not properly defined and does not allow accurate estimation of the cross-sectional area using geometric assumptions. It follows that the accuracy of sonography for the simultaneous assessment of cross-sectional area, flow velocity, and the resulting flow volume can only be marginal. Furthermore, flow measurements performed by using cardiac catheterization and thermal dilution require steady-state hemodynamic conditions, which are difficult to apply to transient changes in flow volume. Hence, these traditional methods do not directly assess real-time blood flow, by which both velocity and cross-sectional area are simultaneously acquired.

Limitations

With real-time EPI data acquisition, the adverse effects of cardiac and respiratory motion on flow measurements can be disregarded. Thus, patients suffering from arrhythmias or dyspnea can be examined. How-

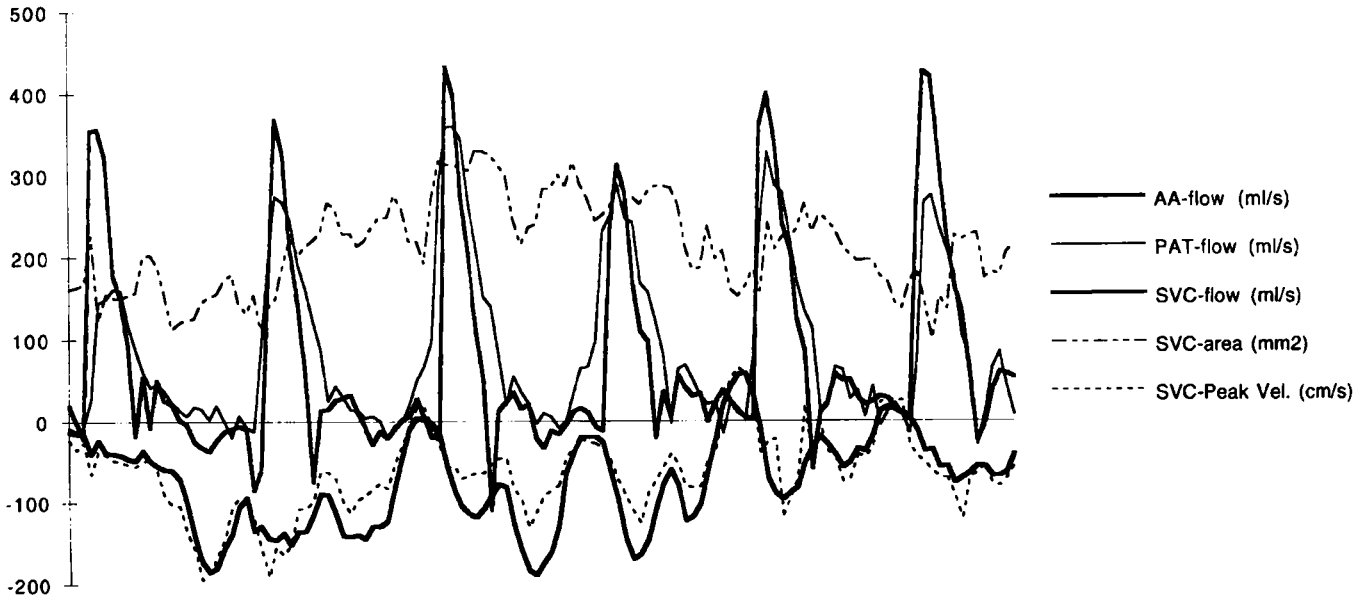

Figure 5. Real-time EPI flow measurements for a period of 5.3 seconds during dynamic strain release in the ascending aorta, pulmonary trunk, and superior vena cava. Strain release coincided with the beginning of the scan.

ever, respiratory motion continues to pose limitations. As mentioned, the technically inadequate imaging of the pulmonary trunk was attributed to respiratory motion through the fixed MR imaging plane. Respiratory motion can be tolerated as long as the translation motion does not move the imaged vessel out of the imaging plane. Whenever imaging is done in the transaxial plane, respiratory motion has only a small effect on vessels, such as the SVC and aorta, oriented in the craniocaudal direction. In contrast, a small degree of respiratory motion moves oblique or tortuous vessels out of the imaging plane.

The phase-contrast EPI technique provides a trade-off between temporal and spatial resolution. In this study a low spatial resolution was tolerated in order to achieve sufficiently high temporal resolution for analyzing complex flow patterns in the SVC. On the basis of theoretical considerations, the applied spatial resolution is tolerable for flow quantification. Flow measurements accurate to better than 10% can be obtained as long as the pixel length is 25% or less than the vessel's diameter. With such large pixels for the estimation of blood flow, it becomes increasingly difficult to evaluate the correct velocity profile. It is the edge pixels, containing both flowing blood and stationary tissue, that introduce relatively gross errors into the estimation of flow and vessel area. The theoretical considerations given here assumed parabolic flow. When assuming plug flow, resulting from stenotic vessels, flow errors were larger. Although in some of the situations encountered in this study (e.g., small cross-sectional area of the SVC during strain) the condition that the cross section of the SVC be smaller than four times the pixel length was not met, the repetitive acquisition of 25 data points in 1 second and their consistency in series can only suggest that the data acquisition scheme is adequate. Although the expected flow patterns were observed in this study, the real-time phase-contrast EPI technique was not validated by an independent imaging technique. Development of such an independent technique in order to confirm the value of EPI for measuring transient flow in vivo remains an area for further research.

• CONCLUSIONS

The application of a new MR imaging technique for evaluating an old clinical intervention has been presented and has directly proved, for the first time, that venous return is reduced during Valsalva's maneuver. In contrast to other techniques, phase-contrast EPI provides direct assessment of transient flow and velocity patterns. Although the real-time measurement of flow in the great vessels is a valuable measurement alone, the MR images also provide a wealth of information on morphology and on the spatial and temporal distribution of velocities in the vessels. To date, this wealth of additional information has not been systematically evaluated. EPI promises to become a useful tool for the study of physiologic and pathologic flow dynamics of the great vessels.

References

1. Gorlin R, Knowles JH, Storey CF. The Valsalva maneuver as a test of cardiac function. Am J Med 1957; 22:197–212.
2. Cohen ML, Cohen BS, Kronzon I. Superior vena caval blood flow velocities in adults: a Doppler echocardiographic study. J Appl Physiol 1986; 61:215–219.
3. Appleton CP, Hatl LK, Popp RL. Superior vena cava and hepatic vein Doppler echocardiography in healthy adults. J Am Coll Cardiol 1987; 10:1032–1039.
4. Sharpey-Schafer EP. Effects of Valsalva's manoeuvre on the normal an failing circulation. Br Med J 1995; 1:693–695.
5. Nishimura RA, Tajik AJ. The Valsalva maneuver and response revisited. Mayo Clin Proc 1986; 61:211–217.
6. Eichenberger AC, Jenni R, von Schulthess GK. Aortic valve pressure gradients in patients with aortic valve stenosis: quantification with velocity-encoded cine MR imaging. AJR 1993; 160:971–977.
7. Kondo C, Caputo GR, Semelka R, Foster E, Shimakawa A, Higgins CB. Right and left ventricular stroke volume measurements with velocity-encoded cine MR imaging: in vitro and in vivo validation. AJR 1991; 157:9–16.
8. Bryant DJ, Payne JA, Firmin DN, Longmore DB. Measurement of flow with NMR imaging using a gradient pulse and phase difference technique. J Comput Assist Tomogr 1984; 8:588–593.
9. Firmin DN, Nayler GL, Klipstein RH, Underwood SR, Rees R, Longmore DB. In vivo validation of magnetic resonance velocity mapping. J Comput Assist Tomogr 1987; 11:751–756.

10. Poncelet BP, Weisskoff RM, Wedeen VJ, Brady TJ, Kantor H. Time of flight quantification of coronary flow with echo planar MRI. Magn Reson Med 1993; 30:781–785.
11. Gatehouse PD, Firmin DN, Collins S, Longmore DB. Real time blood flow imaging by spiral scan phase velocity mapping. Magn Reson Med 1994; 31:504–512.
12. Butts RK, Hangiandreou NJ, Riederer SJ. Phase velocity mapping with real time line scan technique. Magn Reson Med 1993; 29:134–138.
13. Edelman RR, Manning WJ, Gervino E, Li W. Flow velocity quantitation in human coronary arteries with fast breath-hold MR angiography. J Magn Reson Imaging 1993; 3:699–703.
14. Firmin DN, Klipstein RH, Hounsfield GL, Paley MP, Longmore DB. Echo planar high resolution flow velocity mapping. Magn Reson Med 1989; 12:316–327.
15. Guilfoyle DN, Gibbs P, Ordridge RJ, Mansfield RR. Real time flow measurements using echo planar imaging. Magn Reson Med 1991; 18:1–8.
16. McKinnon GC, Debatin JF, von Schulthess GK. On the optimum parameters for rapid phase contrast flow measurements. In: Proceedings of the Society of Magnetic Resonance in Medicine 1994. Berkeley, CA: Society of Magnetic Resonance in Medicine, 1994; 148.
17. Debatin JF, Davis C, Felblinger S, McKinnon GC. Evaluation of ultrafast phase contrast imaging in the thoracic aorta. MAGMA 1995; 3:59–66.
18. McKinnon GC, Koechli V, von Schulthess GK. Towards ultrafast phase contrast MRI with interleaved EPI. In: Proceedings of the Society of Magnetic Resonance in Medicine 1993. Berkeley, CA: Society of Magnetic Resonance in Medicine, 1993; 1264.
19. McKinnon GC. Ultrafast interleaved gradient echo planar imaging on a standard scanner. Magn Reson Med 1993; 30:609–616.
20. McKinnon GC. Interleaved echo planar phase contrast angiography. Magn Reson Med 1993; 31:682–685.
21. McKinnon GC, Debatin JF, Wetter DR, von Schulthess GK. Interleaved echo planar flow quantification. Magn Reson Med 1994; 32:1–5.
22. Wetter DR, McKinnon GC, Debatin JF, von Schulthess GK. Comparison of single shot and multiple shot echoplanar imaging. Radiology 1995; 194:765–770.
23. Gindea AJ, Slater J, Kronzon I. Doppler echocardiography flow velocity measurements in the superior vena cava during the valsalva maneuver in normal subjects. Am J Cardiol 1990; 65:1387–1391.
24. Attubatu MJ, Katz ES, Feit F, Bernstein N, Schwartzman D, Kronzon I. Venous changes occurring during the Valsalva maneuver: evaluation by intravascular ultrasound Am J Cardiol 1994; 74:408–410.